

# Highly resolved measurements of periodic radial electric field and associated relaxations in edge biasing experiments

P. Peleman<sup>a,\*</sup>, Y. Xu<sup>b</sup>, M. Spolaore<sup>c</sup>, J. Brotankova<sup>d</sup>, P. Devynck<sup>e</sup>,  
J. Stöckel<sup>d</sup>, G. Van Oost<sup>a</sup>, C. Boucher<sup>f</sup>

<sup>a</sup> Department of Applied Physics, Ghent University, Rozier 44, 9000 Ghent, Belgium

<sup>b</sup> Laboratory for Plasma Physics, ERM/KMS, B-1000 Brussels, Belgium

<sup>c</sup> Consorzio RFX, Associazione EURATOM-ENEA sulla Fusione, Padova, Italy

<sup>d</sup> Institute of Plasma Physics, Association EURATOM-IPP.CR, Prague, Czech Republic

<sup>e</sup> Association EURATOM-CEA sur la fusion contrôlée, Saint Paul Lez Durance, France

<sup>f</sup> INRS, Institut National de la Recherche Scientifique, Varennes (Que.), Canada J3X 1S2

## Abstract

High time-space resolved measurements of the radial electric field  $E_r$  and plasma rotations have been performed during edge biasing experiments in the CASTOR tokamak. During polarization, edge sheared  $E_r \times B$  flow is routinely generated, triggering a transition to a global improved confinement and a formation of an edge transport barrier (ETB). Furthermore, on top of the biasing-imposed DC  $E_r$ , we observed, for the first time, concurrent fast periodic oscillations (dubbed as relaxations) on  $E_r$ , plasma rotations, edge recycling and the ETB as well. Although the global confinement improvements are not much affected by the relaxation event, the local edge plasma parameters and the ETB are substantially modulated during the oscillating phases. Moreover, throughout the relaxation period a possible link between the modulated radial transport and the toroidal plasma flow is found. The results support the paradigm of the nonlinear dynamical coupling and energy transfer between the turbulence eddies and plasma flows.

© 2007 Elsevier B.V. All rights reserved.

PACS: 52.25.Fi; 52.25.Gj; 52.30.-q; 52.35.-g; 52.40.Hf

Keywords: Relaxations; Edge transport; Plasma flow; Radial electric fields

## 1. Introduction

The importance of the edge radial electric field ( $E_r$ ) and its shear for plasma transport has already been recognized for a long time. Many theoretical

models successfully studied the link between  $E_r$  and the formation of edge or internal transport barriers triggering an improved confinement [1–3]. The transition from low (L-mode) to high confinement (H-mode) can occur spontaneously or can be induced by an externally imposed electric field through edge biasing [4–6]. A biased electrode can drive a radial current in the plasma edge resulting in a  $j_r \times B_\phi$  force and thus a sheared  $E_r \times B_\phi$  poloidal

\* Corresponding author.

E-mail address: [peter.peleman@UGent.be](mailto:peter.peleman@UGent.be) (P. Peleman).

flow, which may suppress turbulence and related transport [7]. Therefore, the radial electric field perturbs the plasma edge and acts as a trigger mechanism to modify the plasma confinement. However, hitherto a thorough understanding of the flow shear and its role in inducing confinement improvements is still a challenge for fusion researchers. Consequently, detailed studies on this subject are still needed.

In this paper, we report the experimental results performed during edge biasing experiments in the Czech Academy of Science Torus (CASTOR) tokamak [8]. In addition to the improvement of global confinement, fast relaxation events on  $E_r$  and related quantities during the biasing phase are also observed for the first time. The paper is organized as follows. In Section 2, we describe the experimental set-up of the biasing experiments. The results and discussions are presented in Section 3. Section 4 gives a summary and conclusions.

## 2. Experimental set-up

Polarization experiments were conducted on the CASTOR tokamak which has a major radius  $R_0 = 40$  cm and a minor plasma radius  $a = 6.6$  cm. An electrode was inserted from the top of the torus well inside the last closed flux surface (LCFS) ( $r/a = 0.6$ ). To create an edge radial electric field  $E_r$  and its shear, a biasing voltage abruptly ramped from 0 to +260 V was applied during the flat-top phase of a discharge, which typically has the following parameters: central chord-averaged plasma density  $\bar{n}_{e,0} = 1.0 \times 10^{19} \text{ m}^{-3}$ , plasma current  $I_p = 12$  kA and  $B_T = 1.3$  T in ohmically heated hydrogen plasmas. A conventional rake probe (radial separation between two adjacent pins = 2.54 mm) and located  $40^\circ$  toroidally from the electrode, was used to simultaneously measure the floating potential  $\phi_f$  and ion saturation current  $I_s$  at various radial positions. A Gundestrup probe, located  $180^\circ$  toroidally from the electrode, was inserted from the top of the vessel to measure the toroidal and poloidal flow velocities. The Gundestrup probe consists of eight collector plates surrounding a cylindrical boron nitride body [9]. The data were digitized at a sampling rate of 1 MHz for both the rake and Gundestrup probe. The  $H_\alpha$  diagnostic is located at the top of the vessel at the same toroidal location as the rake probe to monitor the radiation due to recycling with a sampling frequency of 40 kHz.

## 3. Experimental results and discussions

### 3.1. Global confinement improvement

The effects of the positive edge electrode biasing on the main plasma parameters are shown in Fig. 1 for a time interval of interest (a full discharge duration  $\approx 30$  ms). The figure shows time traces of the electrode voltage ( $V_E$ ) and current ( $I_E$ ), central line-averaged density  $\bar{n}_e$ ,  $H_\alpha$  emission and the ratio of  $\bar{n}_e/H_\alpha$  along with the radial electric field  $E_r$  measured at  $r = 60$  mm by the rake probe (radial derivative of  $\phi_f$  on two adjacent pins). Before biasing, the electrode was grounded so no current flows between the electrode and the vessel. At about 10 ms, a positive biasing voltage  $V_E \approx 260$  V is abruptly applied and maintained constant thereafter for  $\sim 5$  ms, during which a current  $I_E = -20$  A is drawn by the electrode, as seen in Fig. 1(a). In Fig. 1(b), it can be seen that during biasing,  $\bar{n}_e$  is built-up gradually and reached  $1.7 \times 10^{19} \text{ m}^{-3}$  at  $t = 14$  ms before falling off to its original pre-bias value of  $1 \times 10^{19} \text{ m}^{-3}$ .

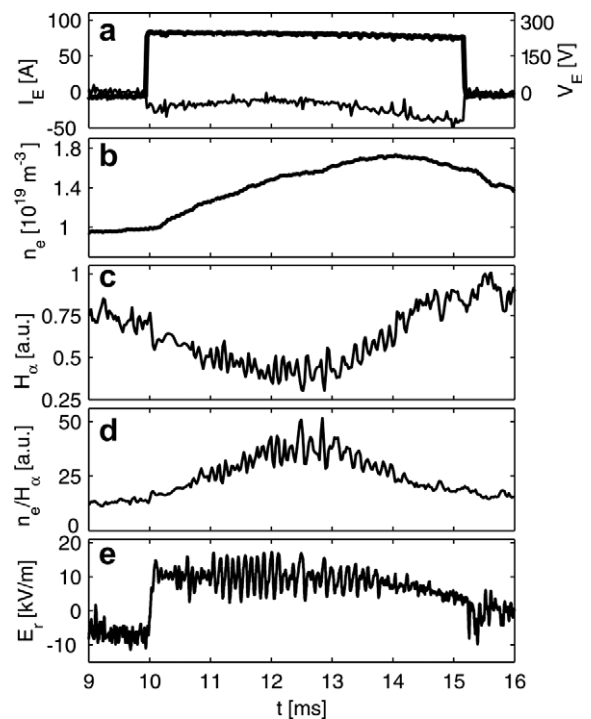


Fig. 1. Time evolution of plasma parameters during a typical edge electrode biasing experiment on CASTOR (shot No. 24076). (a) the electrode voltage  $V_E$  (thick line) and current  $I_E$  (thin line), (b) the central line-averaged electron density  $\bar{n}_e$ , (c)  $H_\alpha$  radiation, and (d) the ratio of  $\bar{n}_e/H_\alpha$ . Shown in (e) is the time trace of the radial electric field measured at  $r = 60$  mm.

In the initial stage of the biasing, from 10 to 12.5 ms, we can see a clear reduction in recycling indicated by a drop in  $H_\alpha$  emission, and thus, a net increase of the ratio  $\bar{n}_e/H_\alpha$  (which is roughly proportional to the particle confinement time  $\tau_p$ ) by a factor of 4 with respect to the pre-bias case. All of these results indicate an improvement of the global particle confinement induced by the electrode biasing, as observed earlier [10]. After 12.5 ms, the  $H_\alpha$  increases simultaneously with the  $C_{III}$  signal (not shown here), suggesting an overheating on the electrode head which contaminates the plasma. In Fig. 1(c)–(e), the signals display periodic oscillations, which will be discussed in Section 3.2. Fig. 2 further illustrates the influence of polarization on the radial dependence of edge plasma equilibrium parameters. In the figures, the radial profiles of the floating potential  $\phi_f$ ,  $E_r$  and its shear  $dE_r/dr$ , and ion saturation current  $I_s$  are obtained by averaging over a time window of 4 ms before (open symbols) and during (filled symbols) the biasing phase. Here,  $E_r$  is calculated directly from the radial derivative of  $\phi_f$  neglecting the contribution from the  $T_e$  gradient, and therefore somewhat underestimated. These approximations are justified due to the very slight changes in edge  $T_e$  and  $\nabla T_e$  before and during the biasing phase observed in similar biasing experiments. In the same context, it is assumed that the  $I_s$  profiles reflect mainly the changes in plasma density as  $I_s \propto nT_e^{1/2}$ . The radial position of the LCFS is around  $r_{LCFS} = 66$  mm (indicated by dashed line

in Figs. 2 and 3). During the biasing phase, the radial dependence of  $\phi_f$  is strongly modified (see Fig. 2(a)), leading to a narrow positive and single-peaked  $E_r$  structure with a maximum of 11 kV/m at  $r \approx 61$  mm, just inside the LCFS (see Fig. 2(b)). As a consequence, a strong positive ( $\sim 1.3$  MV/m<sup>2</sup>) and negative ( $\sim -1$  MV/m<sup>2</sup>)  $E_r$  shear is generated inside and across the LCFS, respectively, as shown in Fig. 2(c). The maximum shear decorrelation rate of the  $E_r \times B$  flow,  $\tau_s^{-1} \propto dv_{E \times B}/dr$ , is thus about  $1\text{--}1.3 \times 10^6$  s<sup>-1</sup>. On the other hand, we have calculated the decorrelation rate of local turbulence scattering,  $\tau_{c0}^{-1}$ , from the e-folding time of the auto-correlation function of  $I_s$  fluctuation data detected before biasing, which gives  $\tau_{c0}^{-1} = 1.6 \times 10^5$  s<sup>-1</sup>. Thus, the flow shear rate significantly exceeds the turbulence decorrelation rate and hence reduces turbulence and turbulent transport [11]. The reduction in  $I_s$  and  $\phi_f$  fluctuations during biasing has been observed in the present experiments. The reduced turbulent transport leads to a formation of the edge pedestal and thus steepening of the edge density profile during biasing, as shown in Fig. 2(d). From all the above facts, we conclude that a clear and reproducible transition to an improved confinement is induced by the edge electrode polarization along with a creation of a particle edge transport barrier just inside the LCFS. This barrier is characterized by a (i) substantial increase of the edge density gradient; (ii) reduction in recycling indicated by a drop in  $H_\alpha$  signal; (iii) substantial increase of the global

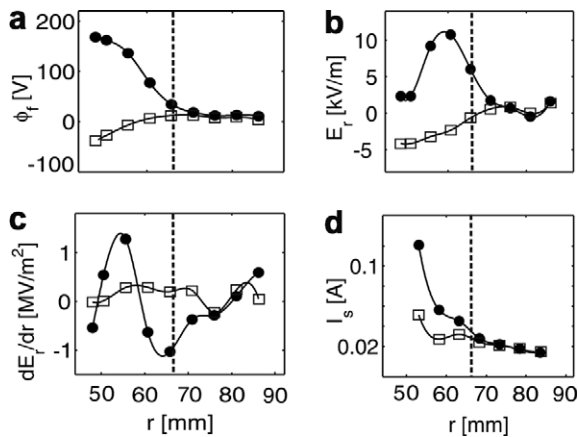


Fig. 2. Radial profiles of (a) the floating potential  $\phi_f$ , (b) the radial electric field  $E_r$ , (c) the  $E_r$  shear, and (d) the ion saturation current  $I_s$  averaged over 4 ms before (open symbols) and during (filled symbols) the polarization, where  $\phi_f$  and  $I_s$  are measured by a rake probe. The vertical dashed line marks the position of the LCFS.

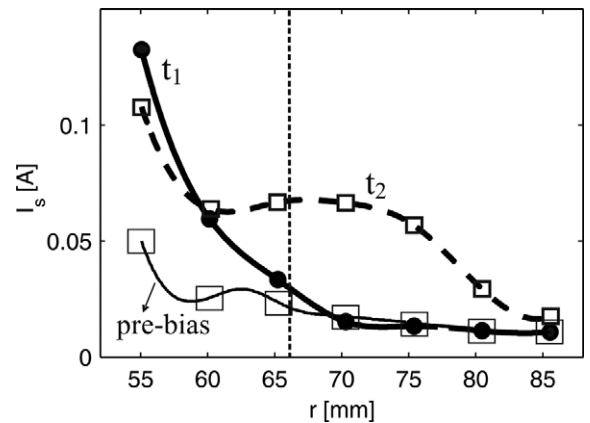


Fig. 3. Radial ion saturation current profiles measured by a rake probe at three different times. The curve of ‘pre-bias’ is the averaged value detected before the biasing phase (the same as in Fig. 2(d)). The other two are the  $I_s$ -profiles measured at times  $t_1$  and  $t_2$  indicated in Fig. 4. The vertical dashed line marks the position of the LCFS.

particle confinement time; (iv) suppression of the density and potential fluctuation level.

### 3.2. Periodic relaxation on $E_r$ and related quantities

In these experiments, an important finding is the periodic relaxation behaviour of  $E_r$  and related quantities during the biasing period. As shown in Fig. 1(e), the  $E_r$  signal in the biasing phase (between 11 and 14 ms) clearly exhibits periodic oscillations ( $f \sim 10$  kHz, amplitude  $7 \text{ kV m}^{-1}$ ) on top of a DC  $E_r$  value ( $\sim 11 \text{ kV m}^{-1}$ ). The concurrent oscillations in  $H_\alpha$  and  $\tau_p$  can also be seen in Fig. 1(c) and (d), respectively. These oscillations do not affect the global confinement properties, since the averaged values of  $H_\alpha$  and  $\tau_p$  evolve continuously with time. Nevertheless, a modulation on the edge transport barrier (ETB) can still be seen from the edge density profile on top of its average level. Plotted in Fig. 3 are the radial dependence of density ( $\propto I_s$ ) at three different times. The reference one (open squares – pre-bias) is the same as that shown in Fig. 2(d),

i.e. the averaged value detected prior to the biasing phase. The other two are measured at time  $t_1$  and  $t_2$ , when the oscillating  $E_r$  is maximum and minimum, respectively, as indicated in Fig. 4. Fig. 3 clearly shows that (i) during biasing the averaged density gradient, i.e., average of profiles of  $t_1$  and  $t_2$ , is much steeper than that of pre-bias profile; (ii) with oscillation of  $E_r$ , the density profiles change from a very steep one at  $t_1$  to a less steep one at  $t_2$ , indicating a modulation of the ETB during the improved confinement stage. Meanwhile, it is found that the edge poloidal and toroidal plasma rotations also oscillate simultaneously with  $E_r$  at the same time period. We dub this phenomenon as a relaxation event (RE). The details of the RE are shown in Fig. 4 for a time window of 0.35 ms. Plotted in Fig. 4 are time traces of  $E_r$ ,  $H_\alpha$ , poloidal ( $v_\theta$ ) and toroidal ( $v_\phi$ ) plasma flow velocities measured at  $r = 60$  mm and  $I_s$  measured at two different radial positions ( $I_{s1}$  at  $r_1 = 53$  mm,  $I_{s2}$  at  $r_2 = 68$  mm) across the ETB region. The absolute value of the density gradient around the transport barrier ( $\propto |\nabla I_s| = |(I_{s2} - I_{s1}) / (r_2 - r_1)|$ ) is shown in Fig. 4(e). In Fig. 4(c),  $v_\theta$  and  $v_\phi$  are deduced from Gundestrup probe measurements using an improved one dimensional fluid probe model in which a constant  $T_e = 35$  eV is assumed [12,13]. From the figures, we can see that  $E_r$ ,  $v_\theta$  and  $|\nabla I_s|$  are changing in phase while  $v_\phi$  and  $H_\alpha$  vary out of the phase with  $E_r$ . The lowest order single ion radial force balance equation  $E_r = \nabla_r P_i / n_i Z_i e - v_{\theta,i} B_\phi + v_{\phi,i} B_\theta$  has been checked using the measured quantities, where  $P_i$  denotes the ion pressure and  $Z_i e$  the electric charge. It has been found that the equation is well verified throughout the oscillation phase. Moreover, the in-phase-oscillations between  $E_r$  and  $v_\theta$  and the out-of-phase-oscillations between  $E_r$  and  $v_\phi$  and  $|\nabla I_s|$  indicate that the diamagnetic term  $\nabla P_i$  alone cannot account for the development of the  $E_r$  oscillations, but are rather dominated by the poloidal flow oscillations. The overall feature of the  $E_r$  relaxation can be further illustrated by a one-period process. First,  $E_r$  increases gradually to its threshold value (18 kV/m) at  $t_1$ . Meanwhile,  $v_\theta$  and  $|\nabla I_s|$  increase, whereas  $H_\alpha$  drops indicating an increase of poloidal sheared flows, decrease of the local particle flux and strengthening of a local transport barrier (see profile at  $t_1$  in Fig. 3). From  $t_1$  to  $t_2$ , with the relaxation of  $E_r$  from its maximum to bottom, the concomitant drop in  $|\nabla I_s|$  and increase in  $H_\alpha$  reveal a fading of the local barrier, as shown also in Fig. 3 by the profile at  $t_2$ . It is interesting to

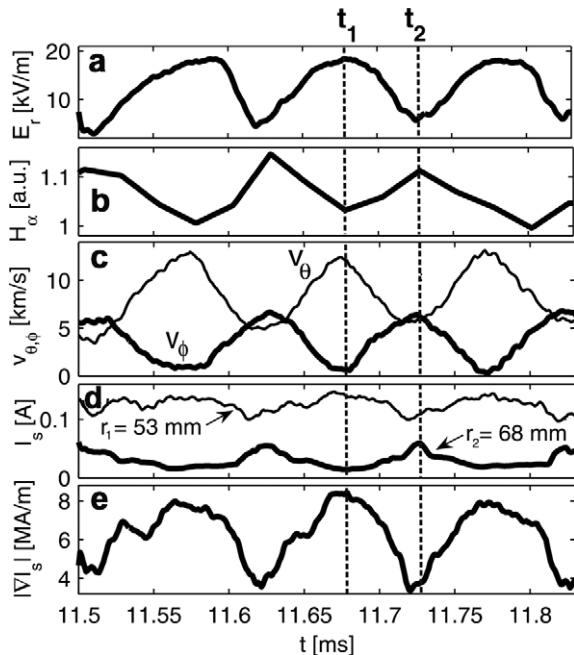


Fig. 4. Time evolution of (a)  $E_r$ , (b)  $H_\alpha$ , (c) poloidal  $v_\theta$  (thin line) and toroidal  $v_\phi$  (thick line) velocities measured at  $r = 60$  mm, (d)  $I_{s1}$  (thin line) and  $I_{s2}$  (thick line) measured by a rake probe at  $r_1 = 53$  mm and  $r_2 = 68$  mm, respectively, and (e)  $|\nabla I_s| = |(I_{s2} - I_{s1}) / (r_2 - r_1)|$  showing oscillations of the signals. The two dashed vertical lines mark the times when a relaxation of  $E_r$  starts ( $t_1$ ) and ends ( $t_2$ ).

see that, throughout the above process, the behaviour of the toroidal flow,  $v_\phi$ , is completely different from that of  $E_r$  and  $v_\theta$ , but follows the variation of the radial transport. For example, from  $t_1$  to  $t_2$ , with the fading of the local transport barrier, the flattening of the edge density profile implies an enhancement of outflux, which may transfer energy to the toroidal flow via dynamical coupling and thus increases  $v_\phi$  substantially. This coupling can occur through the turbulence-driven Reynolds stress. Similar phenomena for the nonlinear dynamical interaction between the turbulent transport and the toroidal flow have been reported on JET [14,15] in non-biasing experiments, where, in particular, the large scale components ( $\sim 12.5$  kHz) show dominant effects. In our case, the periodic link between the turbulent transport and the parallel flow takes place at an almost fixed frequency of  $f \approx 10$  kHz, which is probably triggered by  $E_r$  and interestingly close to the dominant frequencies in JET. Further investigation on the mechanism of the oscillations is still underway.

#### 4. Conclusion

In conclusion, the results of highly resolved spatio-temporal measurements of the edge radial electric field  $E_r$  and plasma rotations during the edge polarization experiments in the CASTOR tokamak have been presented. With biasing, a clear and reproducible transition to an improved confinement is routinely observed along with the formation of an edge transport barrier. Furthermore, we observed for the first time the concurrent fast periodic relaxations on  $E_r$ , plasma rotations, edge recycling and the edge transport barrier during the globally improved confinement phase on top of the biasing-imposed DC  $E_r$ . The oscillation event

does not much affect the global confinement properties, but does modulate the local edge plasma parameters and the transport barrier as well. During the oscillating phase,  $E_r$  and associated quantities well obey the radial force balance  $E_r$ -equation, suggesting a radial equilibrium of the local parameters unaffected in the process. In addition, a possible link between the relaxation of the radial transport and the parallel flow is evidenced during the relaxation process of  $E_r$ , which supports the paradigm of the nonlinear dynamical coupling and energy transfer between the turbulence eddies and zonal (or mean) flows.

#### Acknowledgments

This work was supported by a Fund for Scientific Research-Flanders, Belgium (FWO), and partly by INTAS (Project no. 2001-2056).

#### References

- [1] K.C. Shaing et al., Phys. Fluids B 2 (6) (1990) 1492.
- [2] M. Tendler et al., Comment. Mod. Phys. 2 (N6) (2002) C203.
- [3] M. Van Schoor et al., J. Nucl. Mater. 313–316 (2003) 1326.
- [4] T.E. Stringer, Nucl. Fusion 33 (1993) 1249.
- [5] R.R. Weynants, G. Van Oost, Plasma Phys. Control. Fus. 35 (1993) B177.
- [6] R.R. Weynants et al., Nucl. Fusion 32 (1992) 837.
- [7] G. Van Oost et al., Plasma Phys. Control. Fus. 45 (2003) 621.
- [8] M. Spolaore et al., Czech. J. Phys. 55 (2005) 1597.
- [9] J. Gunn et al., Czech. J. Phys. 51 (2001) 1001.
- [10] G. Van Oost et al., J. Plasma Fus. Res. Series 4 (2001) 29.
- [11] J. Stöckel, in: Proceedings of the 26th EPS Conference on Control Fusion and Plasma Phys, 1999, p. 1589.
- [12] P. Peleman et al., Czech. J. Phys. 55 (2005) 381.
- [13] P. Peleman et al., Contrib. Plasma Phys. 46 (2006) 432.
- [14] C. Hidalgo et al., Phys. Rev. Lett. 91 (2003) 065001.
- [15] C. Hidalgo et al., J. Nucl. Mater. 313–316 (2003) 863.